$Cu_2ZnSn(S,Se)_4$ from Cu_xSnS_y nanoparticle precursors on ZnO nanorod arrays

Jaison Kavalakkatt*[1,2], Xianzhong Lin[1], Kai Kornhuber[1], Patryk Kusch[2], Ahmed Ennaoui[1], Stephanie Reich[2], Martha Ch. Lux-Steiner[1,2]

1) Helmholtz-Zentrum Berlin fuer Materialien und Energie, Hahn-Meitner-Platz 1, D-14109 Berlin, Germany

2) Freie Universitaet Berlin, Berlin, Germany

Abstract

Solar cells with Cu_2ZnSnS_4 absorber thin films have a potential for high energy conversion efficiencies with earth-abundant and non-toxic elements. In this work the formation of CZTSSe from Cu_xSnS_y nanoparticles (NPs) deposited on ZnO nanorod (NR) arrays as precursors for zinc is investigated. The NPs are prepared using a chemical route and are dispersed in toluene. The ZnO NRs are grown on fluorine doped SnO_2 coated glass substrates by electro deposition method. A series of samples are annealed at different temperatures between 300 °C and 550 °C in selenium containing argon atmosphere. To investigate the products of the reaction between the precursors the series is analyzed by means of x-ray diffraction (XRD) and Raman spectroscopy. The morphology is recorded by scanning electron microscopy (SEM) images of broken cross sections. The XRD measurements and the SEM images show the disappearing of ZnO NRs with increasing annealing temperature. Simultaneously the XRD and Raman measurements show the formation of CZTSSe. The formation of secondary phases and the optimum conditions for the preparation of CZTSSe is discussed.

Keywords: kesterite; CZTS; nanoparticle; nanorod; Raman; X-ray diffraction

* Corresponding author: e-mail: jaison.kavalakkatt@helmholtz-berlin.de, jai.k@web.de
Phone: +49 30 8062 42319, Fax: +49 30 8062 43199, Mobile: +49 179 3572588

1 Introduction

Cu_2ZnSnS_4 (CZTS) is a promising nontoxic absorber for solar cells made from earth-abundant elements. With a direct band gap energy of 1.5 eV and a high absorption coefficient (10^4 cm^{-1}) in the visible range CZTS fulfils the requirements for thin film solar cells. $Cu_2ZnSn(S,Se)_4$ (CZTSSe) based devices have already reached an energy conversion efficiency of 10.1 % [1]. With absorber layers made from CZTS nanoparticle (NP) precursors solar cells have reached an energy conversion efficiency of 7.2 % [2]. The NPs disperse in a solution can be deposited by non vacuum methods. The films are then annealed to obtain a compact layer with large grains. For solar cells in superstrate configuration, the absorber thin film can also be deposited on transparent conducting oxide (TCO) layer, e.g. ZnO. With nanostructured TCO the surface can increase many times over. In this work CZTSSe absorber is produced in two steps: (1) ZnO nanorod (NR) arrays are electrodeposited on fluorine doped SnO_2 coated glass substrates (FTO) with a compact ZnO seed layer, followed by a dip coating process of Cu_xSnS_y (CTS) NP. (2) Both serve as precursors during an annealing process in a Se containing atmosphere. A series of samples are prepared at different annealing temperatures. The resulting absorber layers are explored by means of X-ray diffraction and Raman spectroscopy.

2 Experimental details

2.1 Preparation

The method for the preparation of CTS NPs, which are dispersed in toluene, is reported elsewhere [3]. The size of the NPs extracted by means of transmission electron microscopy is 16 ± 3 nm.

The ZnO NR arrays (Fig. 1a) are prepared at 75 °C in an aqueous solution of 7 mM $Zn(NO_3)_2$ and 5 mM NH_4NO_3 by the electro deposition route. The deposition is performed in a three-electrode electrochemical cell with Pt counter and another Pt electrode as reference. FTO is used as working electrode. The deposition is carried at a polarization potential of -1.3 V versus Pt. Further information about the preparation and characteristics of ZnO NR arrays can be found in Ref. [4].

To coat the ZnO NR array with the CTS NPs (Fig. 1b), the substrates with the NRs are dipped in the CTS NP solution. The dipping is performed in three steps with a dip

robot. The substrates are dipped into the solution with a velocity of 8 mm/s, held in the solution for 30 s. The sample is pulled out with 2 mm/s to complete one cycle.

To investigate the formation of CZTSSe during annealing a series of 6 samples is heated between 300 and 550 °C in a tube furnace under Se/Ar atmosphere. The furnace is heated up with 10 °C/min to the set temperature. The given temperature is held for 30 minutes and afterwards the furnace is switched off to cool down to room temperature.

2.2 Analysis

The structural properties of the CZTSSe are investigated by means of X-ray diffraction (XRD) and Raman spectroscopy. The XRD measurements are performed in grazing incidence mode with an incidence angle of 0.9° in a Bruker AXS D8 ADVANCE. A copper X-ray tube is used to measure with the copper Kα line ($\lambda_{K\alpha}$=1.542 Å).

For the Raman measurements a Ti:Sa-ring-laser is used as an excitation. The laser is fully tunable from 690 nm to 1050 nm. To avoid laser heating the beam power is kept below 3.5 mW. Raman spectra are recorded with a Horiba T64000 triple monochromator system in backscattering configuration with a microscope and a motorized XY stage. The micro-Raman spectroscopy with a 100× objective is performed at room temperature with a wavelength of 800 nm.

The morphologies and the compositions of the layers are analyzed in a LEO 1530 GEMINI scanning electron microscope (SEM) of Zeiss. The SEM images are recorded at an acceleration voltage of 10 kV. The energy dispersive X-ray (EDS) measurement are performed in the SEM at an acceleration voltage of 10 kV by a Thermo Noran X-ray silicon drift detector (acquisition and evaluation software Noran System Seven).

Optical measurements are performed with a LAMBDA 950 UV/Vis/NIR Spectrophotometer of PerkinElmer with wavelengths between 250 and 2500 nm.

3 Results and discussion

Cross section images of the ZnO NR array before and after dipping in the CTS solution are shown in Fig. 1a and 1b. The NRs are growing perpendicular to the

rough FTO surfaces. The mean length of the NRs is around 350 ± 50 nm. From top view SEM images a packing density of 76×10^8 cm^{-2} is determined.

After the dipping process, the CTS NPs have filled the space between the NRs, which are completely covered after 4 dips. The NPs form a 300 nm thick top layer. The thickness of this NP layer cannot increase indefinitely, which can also be observed on flat and compact substrates with the same NPs. With the length of the NRs it is possible to control the thickness of the whole layer system. Cross section images of the annealed samples are shown in Fig. 1c - h. During the annealing remaining solvent of the NPs is evaporating and leads to a compact top layer of around 200 nm (Fig. 1c). With increasing annealing temperature the ZnO NR are disappearing. They seem to transform to small particles. After annealing at 500 °C the cross section image cannot provide evidence of ZnO NRs (Fig. 1g). Instead, a double layer with larger crystals on the top of the NPs is obvious. The size of these crystals is increasing after annealing at 550 °C in Se/Ar atmosphere (Fig. 1h). An energy dispersive x-ray measurement in the SEM at the last cross section shows, that Se, S, Zn and Cu are distributed homogeneous in the double layer and Sn has a higher concentration in the bottom layer. The compositions in atom % extract from this measurement is for the top layer: Cu ≈ 20 %, Zn ≈ 30 %, Sn ≈ 6 %, Se ≈ 30%; and S ≈ 10 %; and for the bottom layer: Cu ≈ 16%, Zn ≈ 26%, Sn ≈ 20 %, Se ≈ 26%; and S ≈ 8%. Both layers contain additional carbon (≈ 2 %) and oxygen (≈ 2 %).

Fig. 2 shows the XRD pattern of ‘as deposited’ CTS NPs on ZnO NRs and the annealed samples. The measured peaks are allocated by using the database of the International Centre for Diffraction Data (ICDD) [5].

We observe an evolution of ZnO peaks, which are decreasing with higher annealing temperature. After annealing at 550 °C the ZnO signals disappear. The SnO_2 signals from the FTO are also decreasing slightly with the higher annealing temperatures, but are still present after annealing at 550 °C.

With the ICDD database [5] we allocate Cu_2SnS_3 as well as Cu_3SnS_4 (tetragonal structure), because the peaks are overlapping, as possible CTS phases in our NPs. The Intensity of the CTS main peak (at $2\theta = 28.43$ °) is increasing slightly up to annealing after 400 °C. This peak is shifting to a smaller $2\theta = 28.14$°. Since the diffraction pattern of CTS, ZnS, and CZTS differ a little from each other [5], we conclude that the shift indicates the formation of ZnS or CZTS during the annealing. As the diffraction pattern after annealing at 450 °C shows peaks of CZTSe, the shift

may also caused by the diffusion of Se atoms in the CZTS lattice, which leads to the formation of CZTSSe. This is supported by the fact the intensities of the CZTSe peaks are increasing with higher annealing temperature.

The diffraction pattern after annealing at 550 °C indicates still some CTS, ZnS or CZTS. It can also not be excluded, that ZnSe is formed. The diffraction positions of the ZnSe peaks are similar to the peaks of CZTSe [5]. Other indentified phases shown in Fig. 2 are $CuSeO_4$ [5] after annealing at 350 °C and CuSe [5] after annealing at 500 °C. We observed that the $CuSeO_4$ phase disappears after annealing at 400 °C.

The measured Raman spectra are shown in Fig. 3 for the 'as deposited' as well as the annealed samples between 300 °C and 550 °C. The grey colored circles show the measured and the black solid lines the multi lorentzian fitted spectra. Raman measurements are also performed on a ZnO NR array grown on FTO without NPs. But neither the ZnO NR nor the FTO glass substrate are Raman active at least with an excitation energy of 1.55 eV. The CTS NPs of the 'as deposited' sample show broad Raman peaks at 294 cm^{-1}, 323 cm^{-1} and 349 cm^{-1}. A plateau between 280 and 260 cm^{-1} is also present. By comparison with the work of Fernandes et al. [6] the peaks is allocated to the Raman shifts of Cu_2SnS_3 with cubic (*F*-43*m*) and tetragonal (*I*-42*m*) structures as well as to Cu_3SnS_4 with an orthorhombic (*Pmn*21) structure. We conclude that the main phase in our CTS NPs is Cu_2SnS_3 since the XRD diffractions indicates no orthorhombic and the Raman spectra no tetragonal Cu_3SnS_4 [7].

With increasing annealing temperature these peaks are disappearing in favor of the appearing of CZTS and CZTSe in the Raman spectra. The characteristic main peaks (A_1) of CZTS with a Raman shift of 336 cm^{-1} and of CZTSe with a Raman shift of 198 cm^{-1} are clearly identified after annealing at 450 °C. With increasing temperature next to the main peaks other peaks appear at 235 cm^{-1}, 250 cm^{-1}, 276 cm^{-1}, 298 cm^{-1}, 352 cm^{-1} and 372 cm^{-1}. After annealing at 550°C also a shoulder at the CZTSe peak at 198 cm^{-1} is identified with a Raman shift of 172 cm^{-1}.

The Raman spectra of CZTS layers grown by sulfurization of metallic precursor layers show the main peak at 339 cm^{-1} [8]. These layers also show Raman peaks of CZTS at 287 cm^{-1}, 306 cm^{-1}, 367 cm^{-1} and 375 cm^{-1}. In our layers the peaks at 367 cm^{-1} and 375 cm^{-1} are present in one broad peak at 372 cm^{-1} (Fig. 3). The other broad peak at 298 cm^{-1} is allocated to the other two peaks showed in Ref. [8].

CZTSe thin films prepared by single-stage coevaporation technique show the A_1 peak at 195 cm^{-1} and further peaks at 172 cm^{-1} and 231 cm^{-1} [9]. The small shoulder (172 cm^{-1}) after annealing at 550 °C and the broad peak at 235 cm^{-1} (Fig. 3) are allocated to CZTSe. Since the spectra could not fit with only the CZTS and CZTSe peaks, we conclude that secondary phases are present, indicated by the peaks at 250 cm^{-1}, 276 cm^{-1} and 352 cm^{-1}. These phases are identified as ZnSe (253 cm^{-1}) [10] and ZnS (271 cm^{-1}, 352 cm^{-1}) [11].

Our results on XRD and the Raman measurements at different annealing temperatures confirm the formation of CZTS and CZTSe. From a comparison of our Raman spectra and the one of CZTSSe, prepared with different sulfur to selenium ratios [12], we conclude that CZTSSe is more likely present in our layers. There are several reactions which lead to the formation of CZTSSe. A reaction of the sulfur in the CTS NPs with our ZnO NRs can form ZnS. In the next step CZTS is formed by a reaction of CTS with ZnS, which is described with electroplated precursors to form CZTS [13, 14]. The diffusion of selenium in the CZTS layers can form CZTSSe. The presence of selenium transforms ZnO and ZnS to ZnSe [15, 16]. The ZnSe can also react with the CTS NPs to CZTSSe crystals.

Additional optical measurements of the sample series show an increasing absorption (from approximately 40 to 80 %) of the visible light in favor of a decreased transmission (from approximately 45 to 16 %) . The reflection shows no significant changes in the visible range. The absorption coefficient extract from these measurements is in order of 10^4 to 10^5 cm^{-1}.

4. Conclusions

We prepared CZTSSe by annealing of ZnO NRs coated with CTS NPs. XRD pattern and the Raman spectra show that the CTS NPs react with the ZnO NRs in Se containing atmosphere, resulting in the formation of intermediate phases such as ZnS, ZnSe, $CuSeO_4$. After annealing at 550 °C the dominant phase is CZTSSe. But still secondary phases such as ZnS, ZnSe and CuSe are present in the layer. ZnSe and ZnS are identified by Raman and CuSe by XRD. We believe that the solid state reaction is not completed due the lack of tin to form CZTSSe. To resolve this problem another formulation of the CTS precursor with increasing amount of tin or a better control of the annealing process are required.

Acknowledgement

The work was supported by the BMBF (grant: 03SF0363E).

References

[1] D. A. R. Barkhouse, O. Gunawan, T. Gokmen, T. K. Todorov, D. B. Mitzi, *Prog. Photovolt: Res. Appl.* 20 (2011) 6.

[2] Q. Guo, G. M. Ford, W.-C. Yang, B. C. Walker, E. A. Stach, H. W. Hillhouse, R. Agrawal, *J. Am. Chem. Soc.* 132 (2010) 17384.

[3] X. Lin, J. Kavalakkatt, K. Kornhuber, S. Levcenco, M. Ch. Lux-Steiner, A. Ennaoui, *EMRS 2012 Symposium B, Strasbourg*.

[4] J. Chen, L. Aé, Ch. Aichele, M. Ch. Lux-Steiner, *Appl. Phys. Lett.* 92 (2008) 161906.

[5] International Centre for Diffraction Data (ICDD), ZnO 00-036-1451, SnO_2 00-041-1445, Cu_2SnS_3 00-027-0198, Cu_3SnS_4 00-036-0218, Cu_3SnS_4 00-033-501, ZnS 00-005-0566, Cu_2ZnSnS_4 00-026-0575, $Cu_2ZnSnSe_4$ 04-010-6295, ZnSe 00-037-1463, CuSe 00-027-0185, CuSe 00-034-0171, $CuSeO_4$ 00-017-0842.

[6] P. A. Fernandes, P. M. P. Salomé, A. F. da Cunha, *J. Phys. D: Appl. Phys.* 43 (2010) 215403.

[7] Y. Xiong, Y. Xie, G. Du, H. Su, *Inorganic Chemistry 41* (2002) 2953-2959

[8] P. A. Fernandes, P. M. P. Salomé, A. F. da Cunha, *Journal of Alloys and Compounds* 509 (2011) 7600– 7606.

[9] S. Ahn, S. Jung, J. Gwak, A. Cho, K. Shin, K. Yoon, D. Park, H. Cheong, and J. H. Yun, *Appl. Phys. Lett.* 97 (2010) 021905.

[10] J. Wang, X. H. Liu, Z. S. Li, R. Z. Su, Z. Ling, W. Z. Cai, X. Y. Hou, X. Wang, *Appl. Phys. Lett.* 67 (1995) 2043-2045.

[11] D. N. Talwar, B. K. Agrawal, phys. stat. sol. (b) 64 (1974) 71–78.

[12] E. Mellikov, D. Meissner, M. Altosaar, M. Kauk, J. Krustok, A. Öpik, O. Volobujeva, J. Iljina, K. Timmo, I. Klavina, J. Raudoja, M. Grossberg, T. Varema, K. Muska, M. Ganchev, S. Bereznev, M. Danilson, *Advanced Materials Research* 222 (2011) 8-13.

[13] A. Ennaoui, M. Lux-Steiner, A. Weber, D. Abou-Ras, I. Kötschau, H. –W. Schock, R. Schurr, A. Hölzing, S. Jost, R. Hock, T. Voß, J. Schulze, A. Kirbs, *Thin Solid Films* 517 (2009) 2511-2514

[14] R. Schurr, A. Hölzing, S. Jost, R. Hock, T. Voß, J. Schulze, A. Kirbs, A. Ennaoui, M. Ch. Lux-Steiner, A. Weber, I. Kötschau, H. –W. Schock. *Thin Solid Films* 517 (2009) 2465-2469

[15] D.-C. Perng, J.-F. Fang, J.-W. Chena, *Journal of The Electrochemical Society* 158 (2011) H1097-H1101.

[16] S. Fridjine, S. Touihri, K. Boubaker, M. Amlouk, Journal of Crystal Growth 312 (2010) 202–208

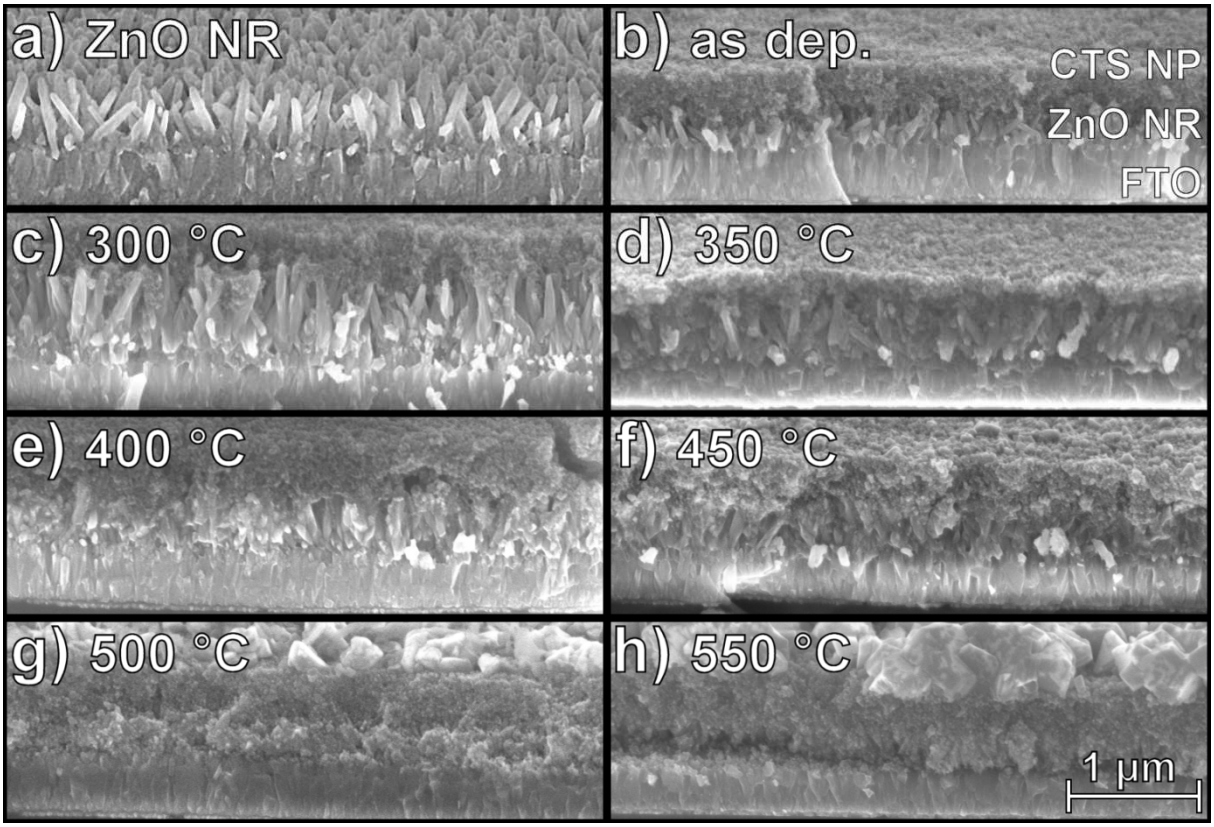

Figure 1:

SEM Images of broken cross sections. The images show a) ZnO NR array deposited via electro deposition, b) ZnO NR array covered with CTS NP after dip coating, c) - h) Layers after annealing at temperatures between 300 and 550 °C of ZnO NR arrays covered with CTS NP.

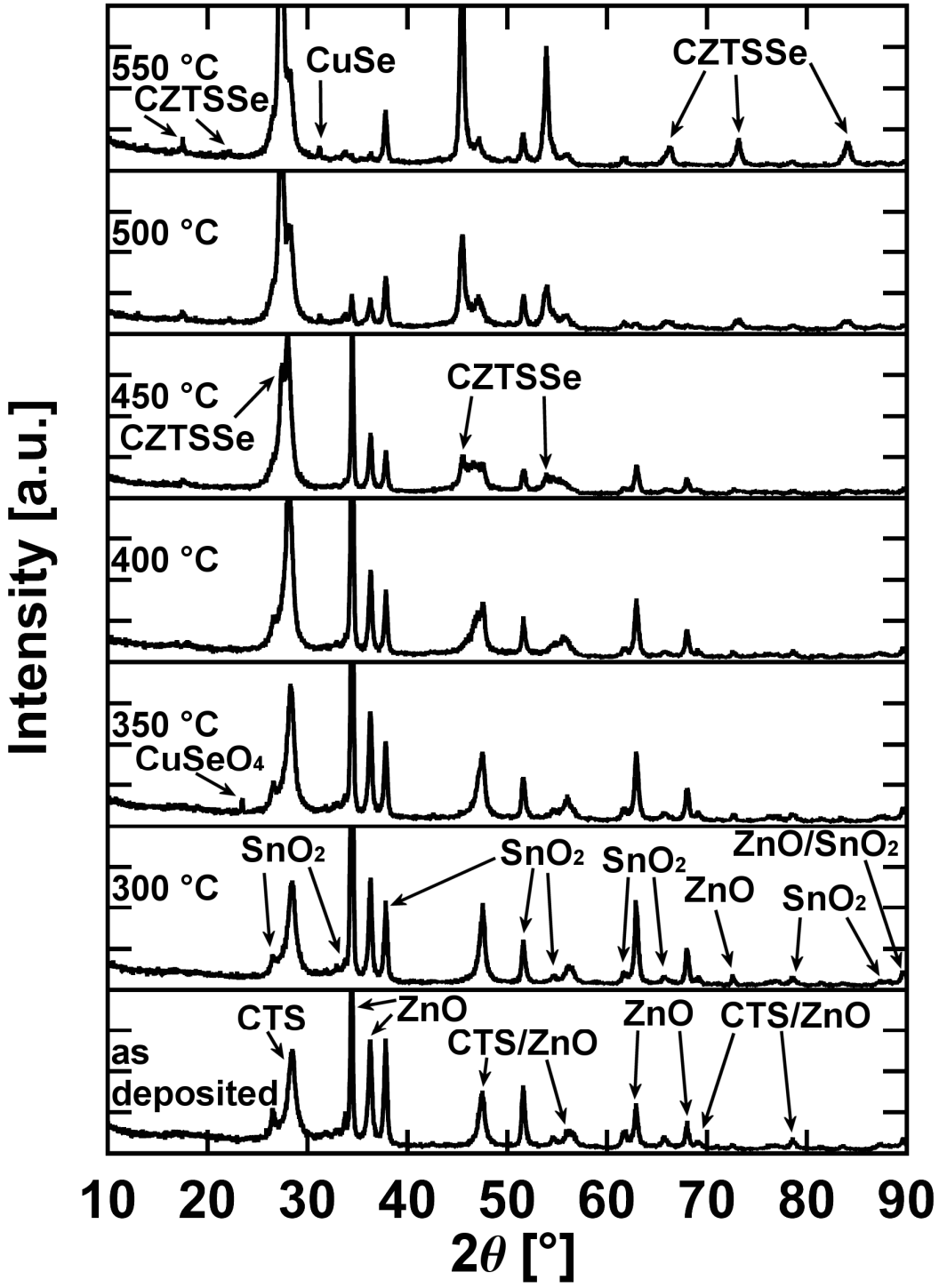

Figure 2:

XRD patterns of not annealed ZnO NR covered with CTS NP (as deposited) and after annealing between 300 and 550°C in selenium containing atmosphere. With increasing annealing temperature CZTSe is present in the layers and ZnO is disappearing. Secondary phases of CuSe (after annealing at 500 and 550 °C) and $CuSeO_4$ (after annealing at 350 °C) are identified.

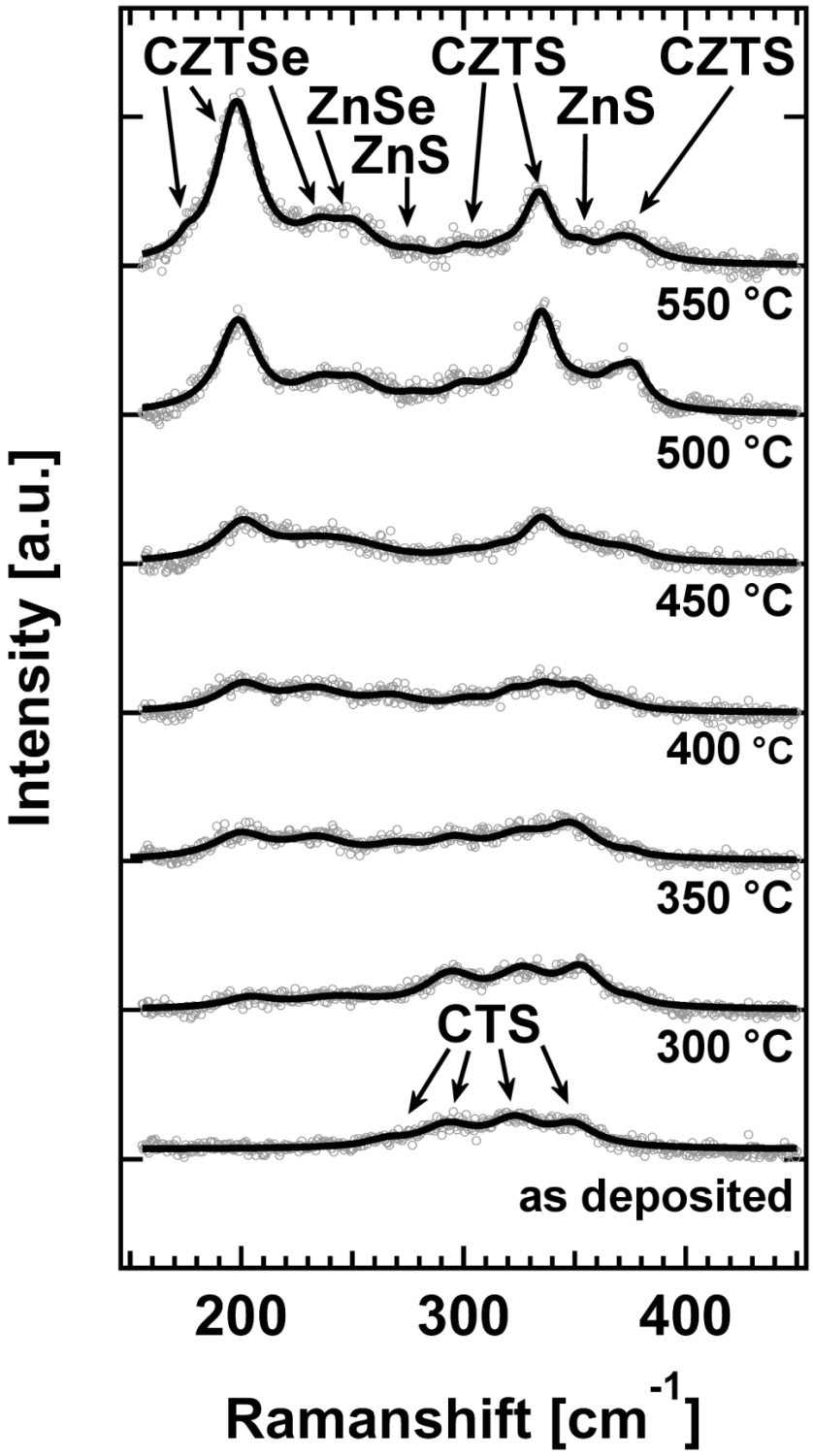

Figure 3:

Raman spectra of not annealed ZnO NR covered with CTS NP (as deposited) and after annealing between 300 and 550°C in selenium containing atmosphere. The grey colored circles show the measured and the black solid lines the fitted spectra. With increasing temperature CZTS and CZTSe are present in the layers. Secondary phases of ZnS and ZnSe are indicated.